Biosensors and Bioelectronics 54 (2014) 15–19

Contents lists available at ScienceDirect

Biosensors and Bioelectronics

journal homepage: www.elsevier.com/locate/bios

Short communication

A single fluorescent protein-based sensor for *in vivo* 2-oxogluatarate detection in cell

Chang Zhang, Bang-Ce Ye*

Lab of Biosystems and Microanalysis, State Key Laboratory of Bioreactor Engineering, East China University of Science & Technology, Shanghai 200237, China

ARTICLE INFO

Article history:
Received 9 September 2013
Received in revised form
13 October 2013
Accepted 22 October 2013
Available online 31 October 2013

Keywords:
Genetically encoded biosensor
2-Oxoglutarate
Nitrogen metabolism
In vivo detection

ABSTRACT

2-Oxoglutarate (2OG) is an important currency stands at the crossroad between carbon and nitrogen metabolism. Recent research found that 2OG acts as a signal in the regulation of nitrogen metabolism in prokaryote. While in eukaryotic cells, 2OG is also attractive since tricarboxylic acid cycle (TCA cycle) in tumor cells was found to undergo metabolic alterations such as the Warburg effect. A method of tracing this key metabolite 2OG at the cellular level is highly desirable. In order to visualize and monitor 2-oxoglutarate metabolism in single living cells, we developed a novel sensor by inserting the functional 2OG-binding domain GAF of the NifA protein into YFP. This sensor was found to be highly specific to 2OG. Following binding of 2OG, fluorescence intensity of the sensor increased with increasing 2OG concentration and reached a 1.5-fold maximum fluorescence signal change (F/F_0-1), kinetics of fluorescence signal upon 2OG association with sensor was fast, the dynamic response range of the mOGsor sensors was 100 μM–100 mM. Dissociation between sensor and 2OG was verified both *in vitro* and *in vivo*. This sensor reported cellular 2OG dynamics in *E. coli* cells in real time upon different nutrition challenges and manifested the differences in 2OG pool accumulation and consumption rate.

1. Introduction

In a wide range of Bacteria and Archaea, the presence of 2OG has been considered critical for cell signaling, in addition to being an important metabolite of the highly conserved Krebs cycle (Zhao et al., 2010). While in human body, 2OG was regarded as a potent protective factor involved in the development of malignant cells (Harrison and Pierzynowski, 2008). Tracking of 2OG in real-time would be useful for studies on deciphering cell metabolism and signal transduction. In the past decade, there have been efforts to directly measure and visualize metabolites in cell by using genetically encoded fluorescence resonance energy transfer (FRET)-based biosensors (Zhang et al., 2013a). And recently, we developed a genetically encoded 2OG biosensor based on fluorescent resonance energy transfer by inserting the functional 2OG-binding domain GAF (Little and Dixon, 2003) of the NifA protein between the FRET pair yellow fluorescent protein and cyan fluorescent protein (Zhang et al., 2013b).

Biosensors based on circularly permuted fluorescent protein (cpFP) have been attractive since they may appear more obvious signal changes in contrast with those based on FRET (Zhao et al., 2011). Proteins can tolerate circular permutation, which produces novel N- and C-termini from different portions of the protein while maintaining a stable structure. Tsien and coworkers, while studying a circular permutation and receptor insertion within the green fluorescent proteins (GFP) (Baird et al., 1999), showed that GFP is surprisingly robust, thus providing a new strategy for creating genetically encoded indicators. Those single color fluorescent indicators (Kawai et al., 2004; Mizuno et al., 2007) consist of a recognition module that specifically response to a ligand and fluorescent proteins (Ormo et al., 1996) as the signal emission part. Conformational changes caused by ligand binding to this recognition module effect fluorophores, resulting in the fluctuation of fluorescence intensity when the domain is placed in a sensitive region of the chromophore. Zhao et al. recently developed cpYFP-based sensors for NADH and monitored the dynamic changes in NADH levels in the organelles of mammalian cells (Zhao et al., 2011). They also investigated the differences in NADH concentration in response to environmental changes in different subcellular compartments showing that genetically encoded indicators can be targeted to subcellular compartments to specifically analyze concentration changes within a specific compartment of an intact live cell. Those successfully generated indicators have shed light on future work.

In attempt to achieve a more sensitive sensor, we utilized the GAF domain to insert into YFP and cpYFP to create biosensors and only the former exhibited a fluorescent signal, the latter was expressed as inclusion body in *E. coli* cells. As a mono-fluorescent

* Corresponding author. Tel./fax: +86 21 64252094.
E-mail address: bcye@ecust.edu.cn (B.-C. Ye).

0956-5663/$ - see front matter © 2013 Elsevier B.V. All rights reserved.
http://dx.doi.org/10.1016/j.bios.2013.10.038

indicator in contrast with FRET biosensors which contain two fluorophores (Oku et al., 2013), this sensor was termed mOGsor. In the presence of ligands, the sensor showed great selectivity and exhibited a concentration-dependent increase in fluorescent intensity with 2OG. This reporter, showed a larger signal change and faster kinetics than the previous FRET sensor (Zhang et al., 2013b), revealed the cellular 2OG dynamics in *E. coli* cells upon metabolic challenges.

2. Materials and methods

2.1. Plasmid generation

The *Nco* I and *Hind* III restriction sites, in the pET-28a (+) vector were used to construct a single-chain biosensor. YFP fragments were cloned from commercial plasmids pEYFP-N1 (Clontech Catalog #6006-1). A candidate gene encoding the 2OG reaction domains of GAF included in the NifA-encoding gene (*NC_012560.1*) was amplified from the genome of *Azotobacter vinelandii* (strain number 10088), which was purchased from the Agricultural Culture Collection of China (ACCC), Beijing, by Polymerase Chain Reaction (PCR) amplification (TakaRa, Japan). Restriction endonucleases were from New England Biolabs (Ipswich, MA). All chemicals, including 2OG, L-glutamic acid, succinate, malate, fumarate and L-glutamine, were of analytical grade, and were purchased from Amresco (Solon, OH). Alanine transaminase (ALT), L-alanine and pyruvate were purchased from Sigma-Aldrich. *E. coli* DH5α, used as the cloning host, and *E. coli* BL21 (DE3)pLysS, used as the protein production host, were purchased from TransGen Biotech (Beijing, China).

2.2. In vitro assays

E. coli BL21 (DE3) pLysS expressing mOGsor were grown for 3 h in 50 mL LB medium (aerobic culture) at 37 °C till the OD reached 0.6 before induction by the addition of 0.5 mM isopropyl-β-D-thiogalactopyranoside (IPTG) overnight. Cells were harvested by centrifugation at 5000*g*, washed twice in 50 mM PBS (pH=8.0) and then resuspended in the same buffer. The cell pellet was suspended in 50 mM PBS (pH=8.0) buffer before sonication, and all the analytes were dissolved in the same buffer and adjusted to a final pH of 8.0. Sensors were purified by His-Bind affinity chromatography (Novagen) and dialyzed against 50 mM PBS (pH=8.0) prior to any *in vitro* assays. Fluorescence was measured using a fluorescence microplate reader (Bio-Tek Instrument, Winooski, VT) and a black 96-well microplate (Fluotrac 200, Greiner, Germany). Emission wavelengths of 522 nm, or a continuous spectrum from 520 to 600 nm, were monitored at the 500 nm excitation, and the excitation spectra were measured at 600 nm. The purified sensor protein was adjusted to be 9 μM and all the detection was carried out at 37 °C. The blank measurement was obtained from a well containing only mOGsor in 50 mM PBS (pH=8.0) buffer. The dissociation constants (K_d) were determined by fitting the fluorescence intensity curves to a single-site-binding isotherm: $I=I_{apo}+(I_{sat}-I_{apo})\times X/(K_d+X)$ (Ewald et al., 2011), under the following parameters: X, ligand concentration; I, fluorescence intensity; I_{apo}, fluorescence intensity in the absence of ligand; and I_{sat}, fluorescence intensity at satufluorescence intensity with ligand. All values were derived from the averages of at least 3 titration experiments.

2.3. 2OG depletion in vitro

Sensors were purified as described earlier and dialyzed against 50 mM PBS (pH=7.6) dissolving 500 mM L-alanine. The 2OG depletion reaction was carried out at 37 °C with 5 mM 2OG and 100 units ALT per cell in 96-well plate. The sensor itself, and the sensor with 100 units ALT were detected simultaneously as control groups.

2.4. In vivo assays

E. coli BL21 (DE3) pLysS expressing mOGsor were cultivated as mentioned earlier. The cells were then starved in carbon-free M9 medium (Ewald et al., 2011) containing 50 mg/L kanamycin sulfate

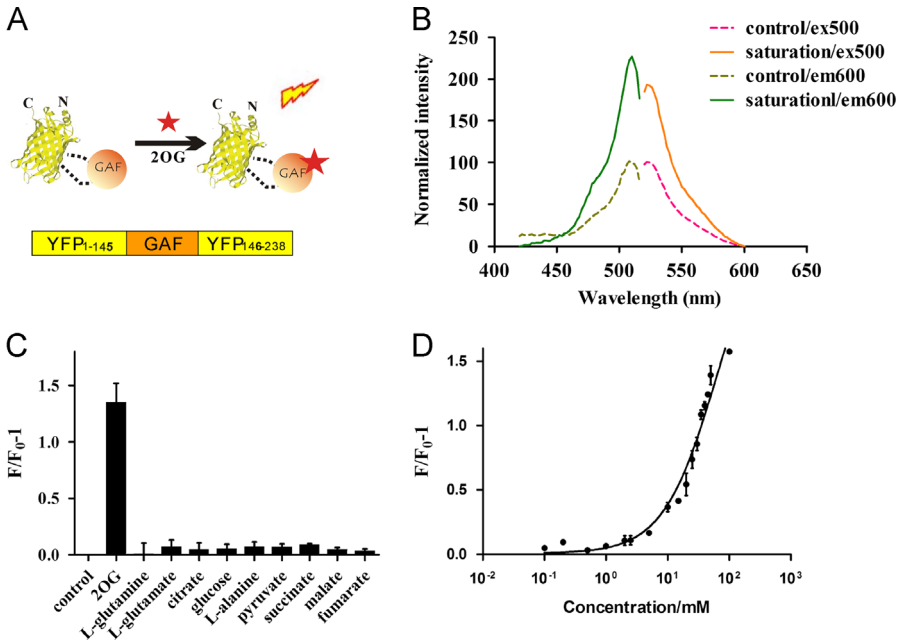

Fig. 1. Properties of the mOGsor *in vitro*. (A) Schematic demonstrating the sensor design, with a GAF domain inserted into YFP and an increase of fluorescence upon binding of 2OG. (B) Fluorescence spectra of purified mOGsor. (C) MOGsor shows high specificity for 2OG at a high concentration (fumarate was detected at 1 mM and others at 100 mM). (D) Binding curve of 2OG with mOGsor. The emission fluorescent intensity was determined at different 2OG concentrations. Error bars indicate standard deviations ($n=3$).

for 4 h at 37 °C to deplete nutrition. 190 μL cultures were transferred to 96-well plates and fluorescence intensity was measured in the fluorescence microplate reader (Bio-Tek Instrument, Winooski, VT) using black 96-well microplates (Fluotrac 200, Greiner, Germany). Subsequently, compounds (all final concentrations of 10 mM), or carbon-free M9 was added to the cultures. The fluorescence intensity before and after the addition of compounds was determined using a fluorescence microplate reader and shaking at 170 rpm between readings. The fluorescence emission at 522 nm (excitation wavelength, 500 nm; bandwidth, 2 nm) was recorded.

3. Results and discussion

3.1. Design and characterization of sensor

To develop a sensor for real-time monitoring of 2OG *in vivo*, we focused on the GAF domain for its specific binding of 2OG and conformational change (Little and Dixon, 2003). Hung et al. inserted a cpFP variant of T-Sapphire into a tandem dimer of Rex from *Thermus aquaticus* to engineer an NADH biosensor (Hung et al., 2011). In our situation, since GAF is a monomeric domain, we decided to insert GAF into YFP between Y145 and N146 (Fig. 1A). Gene segments of GAF and YFP were tandem fused by SOE-PCR (Vallejo et al., 2008) and then expressed in *E. coli* BL21 (DE3) pLysS. To study the fluorescence spectra of purified mOGsor, the excitation spectrum was recorded at an emission wavelength of 600 nm and the excitation peak was 508 nm. Emission spectrum was recorded at an excitation wavelength of 500 nm and has a maximum at 522 nm (Fig. 1B). The addition of 2OG resulted in an increase in both emission and excitation peaks, which demonstrates that the conformation change in the 2OG-recognition domain GAF is translated into a change in fluorescent intensity (Fig. 1A).

To test the specificity of the mOGsor for 2OG, a panel of related metabolite compounds consisting of citrate, glucose, L-glutamate, L-glutamine, L-alanine, succinate, malate, fumarate and pyruvate was applied to the sensor. Our sensor was highly selective for 2OG and did not exhibit apparent fluorescent intensity changes in the presence of other metabolites (Fig. 1C) even when they were at a high concentration (100 mM) considering their physiological concentration ranges in *E. coli* (Bennett et al., 2009). In this test, only fumarate was detected at 1 mM due to the solubility problem.

When the 2OG concentration was increased from 100 μM to 100 mM, the emission fluorescent intensity for the mOGsor increased 1.5-fold, following sigmoid curves (Fig. 1D), the dynamic response range of the mOGsor sensors was 100 μM–100 mM. The dissociation constant (K_d) values was found to be 62.4 mM. Although this dissociation constant exceed regular 2OG concentration *in vivo*, mOGsor still get a 30% uplift in emission fluorescent intensity when effected with 10 mM 2OG, which is detectable in contrast with signal changes of other sensors (Okumoto et al., 2005).

3.2. Dissociation between sensor and 2OG

A feasible sensor should bind to ligands reversibly and recover the initial signal after depletion of the ligand. In order to verify the reversible binding between sensor and ligands, we carried out dissociation analysis both *in vitro* and *in vivo*. Alanine transaminase (ALT), which catalyzes the formation of pyruvate and L-glutamate with 2OG and L-alanine as substrates, was chosen to deplete 2OG *in vitro*. One millimolar of 2OG was added to the detection groups and ALT was added after signal stabilization at 10 min (Fig. 2A). The fluorescence intensity in the sensor/2OG/ALT group got a time-dependent reduction after addition of ALT, and the signal returned to the same as that of control groups without 2OG. In contrast, while sensor/2OG group without ALT addition exhibited a stable and higher fluorescence intensity, ensuring that the sensor was not photobleached after continuous excitation. The other control group, that of sensor/ALT, appeared identical to the sensor without any additions, excluded any possible effect of ALT on sensor.

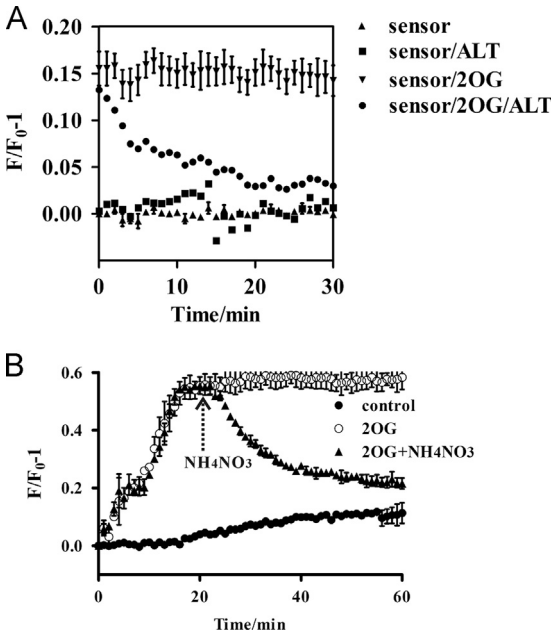

Fig. 2. (A) Monitoring of dissociation between sensor and 2OG *in vitro*. (B) Monitoring of dissociation between sensor and 2OG *in vivo*.

We further monitored 2OG depletion in *E. coli* cells (Fig. 2B). The effect of carbon on cellular 2OG levels was investigated first using a medium-shift scheme. *E. coli* BL21 (DE3) pLysS cells expressing mOGsor in LB medium were transferred to carbon-free M9 medium which was clear in composition, and exhibited no fluorescence signal when excited at 500 nm. After addition of 10 mM 2OG, fluorescence intensity was enhanced and reached a stable state at about 20 min. 2OG, together with NH_4^+, can be transformed to glutamate by GDH (glutamate dehydrogenase) *in vivo*, and $NH_4^+NO_3$, which itself did not effect mOGsor *in vitro* or *in vivo*, was added at 20 min. This resulted in a reduction in the signal intensity over time suggesting that mOGsor was dissociated from 2OG as the 2OG concentration was reduced.

3.3. 2OG dynamics in E. coli cells upon metabolic challenges

Genetically encoded fluorescent sensors allow for the collection of real-time data to study the kinetics of metabolite accumulation. In this study, we also tested the ability of the mOGsor to detect intracellular 2OG levels in living *E. coli* cells *in vivo* under different culture conditions. Firstly, to determine the kinetics of 2OG binding to the biosensor, we monitored the response every 10 s until the signals plateaued. 2OG association with mOGsor was rapid, with a time constant of 155 s at 28 °C, which appears slightly faster, with a time constant of 135 s at 37 °C (Fig. 3A). This mOGsor exhibited fast signal kinetics and a higher fluorescence change than using a FRET-based biosensor with GAF domain sandwiched between YFP and CFP, as previously published by our group (Zhang et al., 2013b). Using this time constant, we carried out studies employing real-time monitoring of 2OG metabolism *in vivo* with different carbon and nitrogen sources.

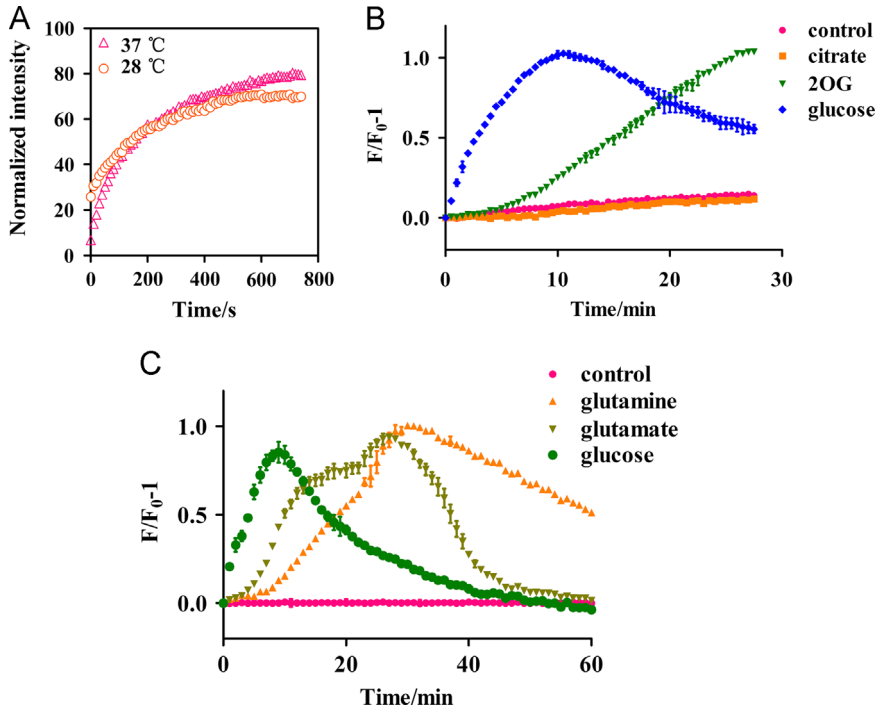

Fig. 3. (A) Kinetics of fluorescence signal upon addition of 2OG at 28 °C and 37 °C. (B) Real time monitoring of different carbon sources addition *in vivo*. (C) Real time monitoring of nanosensor discriminate carbon source addition from nitrogen source addition *in vivo*.

As mentioned previously, all the metabolites (Fig. 1C) analyzed did not effect the mOGsor *in vitro*. Glucose, as a favored carbon source, can be converted to 2OG through the glycolysis pathway and Krebs cycle. Therefore, we next monitored the dynamics of 2OG levels in *E. coli* cells after the addition of exogenous citrate and glucose. Citrate was used as the control for the fluorescence monitoring experiments, since *E. coli* cells do not metabolize citrate as a carbon source under aerobic conditions (Pos et al., 1998). Citrate and glucose were added at concentrations of up to 10 mM to the *E. coli* cells in M9 medium. Fig. 3B shows the time-dependent change in the emission fluorescence intensity following the addition of carbon compounds. The addition of glucose induced a rapid enhancement of fluorescence intensity that peaked at about 10 min and then slowly decreased. As expected, glucose was immediately internalized and metabolized through glycolysis, which then activated the Krebs cycle. These results suggest that the 2OG pool quickly accumulated in response to glucose availability. The slow decrease in the 2OG levels was likely the result of exhausting the supply glucose. In contrast to the results for glucose, the addition of citrate had almost no effect on intracellular 2OG levels. Moreover, the addition of 2OG induced a much slower signal increase compared to glucose addition, indicating that 2OG uptake in *E. coli* cells is not as fast as glucose. Considering the complicated *in vivo* environment, we also used *E. coli* cells expressing YFP as a negative control that showed no obvious fluorescence intensity upon the addition of carbon sources to exclude the possibility of a direct effect of the chromophores.

2OG, together with glutamate and glutamine, constitute a small circulation emphasizing metabolism of both carbon and nitrogen sources (Leigh and Dodsworth, 2007). Therefore, we intended to study the effect of nitrogen sources on 2OG metabolism. *E. coli* cells after starvation can immediately respond to nitrogen sources (Fig. 3C), consuming glutamate and glutamine to produce 2OG as a carbon source. The 2OG pool reached a peak at about 14 min and another peak at 26 min, suggesting that *E. coli* cells might have more than one mechanism for glutamate metabolism, while the 2OG pool in the glutamine addition group peaked at about 30 min indicating that 2OG production from glutamate is faster than that from glutamine. This is in accordance with the fact that glutamine would be deaminated to produce glutamate and then 2OG. The depletion rate of the 2OG pool in the glutamate addition group was faster than that in the glucose group, raising the possibility that, in the glutamate addition group, 2OG went to other pathways besides the TCA.

4. Conclusion

In the present study, to monitor intracellular 2OG levels, the 2OG-binding GAF domain of the NifA protein was inserted into YFP. Our results illustrate that mOGsor is a powerful tool for evaluating the signal transduction and cross-talk mechanisms of central carbon and nitrogen metabolism in relation to the nutritional states of the cell. Other important elements such as glutamate (Hires et al., 2008) and glutamine (Gruenwald et al., 2012) from nitrogen metabolism and citrate (Ewald et al., 2011) from the Krebs cycle have already been exploited by genetically encoded fluorescent biosensors. It is therefore attractive to detect changes in 2OG levels to shed further light on carbon and nitrogen metabolism.

Acknowledgments

This study was supported by the China NSF (21276079, 21335003), SRFDP (No. 20120074110009), the Key Grant Project (No. 313019) of the Chinese Ministry of Education, and the Fundamental Research Funds for the Central Universities.

References

Baird, G.S., Zacharias, D.A., Tsien, R.Y., 1999. Proc. Natl. Acad. Sci. USA 96, 11241–11246.
Bennett, B.D., Kimball, E.H., Gao, M., Osterhout, R., Van Dien, S.J., Rabinowitz, J.D., 2009. Nat. Chem. Biol. 5, 593–599.

Ewald, J.C., Reich, S., Baumann, S., Frommer, W.B., Zamboni, N., 2011. PLoS One 6, e28245.
Gruenwald, K., Holland, J.T., Stromberg, V., Ahmad, A., Watcharakichkorn, D., Okumoto, S., 2012. PLoS One 7, e38591.
Harrison, A.P., Pierzynowski, S.G., 2008. J. Physiol. Pharmacol. 59 (Suppl 1), 91–106.
Hires, S.A., Zhu, Y., Tsien, R.Y., 2008. Proc. Natl. Acad. Sci. USA 105, 4411–4416.
Hung, Y.P., Albeck, J.G., Tantama, M., Yellen, G., 2011. Cell Metab. 14, 545–554.
Kawai, Y., Sato, M., Umezawa, Y., 2004. Anal. Chem. 76, 6144–6149.
Leigh, J.A., Dodsworth, J.A., 2007. Annu. Rev. Microbiol. 61, 349–377.
Little, R., Dixon, R., 2003. J. Biol. Chem. 278, 28711–28718.
Mizuno, T., Murao, K., Tanabe, Y., Oda, M., Tanaka, T., 2007. J. Am. Chem. Soc. 129, 11378–11383.
Oku, M., Hoseki, J., Ichiki, Y., Sakai, Y., 2013. FEBS Lett. 587, 793–798.
Okumoto, S., Looger, L.L., Micheva, K.D., Reimer, R.J., Smith, S.J., Frommer, W.B., 2005. Proc. Natl. Acad. Sci. USA 102, 8740–8745.
Ormo, M., Cubitt, A.B., Kallio, K., Gross, L.A., Tsien, R.Y., Remington, S.J., 1996. Science 273, 1392–1395.
Pos, K.M., Dimroth, P., Bott, M., 1998. J. Bacteriol. 180, 4160–4165.
Vallejo, A.N., Pogulis, R.J., Pease, L.R., 2008. CSH Protocols, pdb prot4861.
Zhang, C., Wei, Z.H., Ye, B.C., 2013a. Biotechnol. J. 8, http://dx.doi.org/10.1002/biot.201300001. (2013).
Zhang, C., Wei, Z.H., Ye, B.C., 2013b. Appl. Microbiol. Biotechnol. 97, 8307–8316.
Zhao, M.X., Jiang, Y.L., He, Y.X., Chen, Y.F., Teng, Y.B., Chen, Y., Zhang, C.C., Zhou, C.Z., 2010. Proc. Natl. Acad. Sci. USA 107, 12487–12492.
Zhao, Y., Jin, J., Hu, Q., Zhou, H.M., Yi, J., Yu, Z., Xu, L., Wang, X., Yang, Y., Loscalzo, J., 2011. Cell Metab. 14, 555–566.